AIP Advances

Nonlinear optical localization in embedded chalcogenide waveguide arrays

Mingshan Li, Sheng Huang, Qingqing Wang, Hrvoje Petek, and Kevin P. Chen

Citation: AIP Advances **4**, 057120 (2014); doi: 10.1063/1.4879619
View online: http://dx.doi.org/10.1063/1.4879619
View Table of Contents: http://scitation.aip.org/content/aip/journal/adva/4/5?ver=pdfcov
Published by the AIP Publishing

AIP ADVANCES **4**, 057120 (2014)

Nonlinear optical localization in embedded chalcogenide waveguide arrays

Mingshan Li,[1] Sheng Huang,[1] Qingqing Wang,[1] Hrvoje Petek,[2] and Kevin P. Chen[1,a]

[1]*Department of Electrical Engineering, University of Pittsburgh, Pittsburgh, Pennsylvania 15261, USA*

[2]*Department of Physics and Astronomy, University of Pittsburgh, Pittsburgh, Pennsylvania 15260, USA*

(Received 14 March 2014; accepted 13 May 2014; published online 21 May 2014)

We report the nonlinear optical localization in an embedded waveguide array fabricated in chalcogenide glass. The array, which consists of seven waveguides with circularly symmetric cross sections, is realized by ultrafast laser writing. Light propagation in the chalcogenide waveguide array is studied with near infrared laser pulses centered at 1040 nm. The peak intensity required for nonlinear localization for the 1-cm long waveguide array was 35.1 GW/cm^2, using 10-nJ pulses with 300-fs pulse width, which is 70 times lower than that reported in fused silica waveguide arrays and with over 7 times shorter interaction distance. Results reported in this paper demonstrated that ultrafast laser writing is a viable tool to produce 3D all-optical switching waveguide circuits in chalcogenide glass. [http://dx.doi.org/10.1063/1.4879619]

An important lightwave architecture for all-optical switching is to utilize spatial soliton schemes in optical waveguide arrays built in nonlinear optical substrates.[1,2] Chalcogenide glasses (GhGs)[3,4] are a class of important optical materials known for their large nonlinear refractive index, wide transparent wave window that spans from visible to mid-infrared, and negligible two photon absorption (TPA) and free carrier generation at the telecom wavelength. These attractive material traits lead to a large nonlinear figure of merit (FOM) for chalcogenide glasses for all-optical signal processing applications. Kerr spatial soliton has been demonstrated in a slab ChG waveguide fabricated by thin-film deposition.[5] Moreover, a number of nonlinear waveguide devices in ChG have been realized through fabrication techniques based on thin-film deposition and various lithography schemes.[6–8] However, the current thin-film deposition and lithography techniques cannot produce multi-layer ChG waveguide structures, which are required for more complex optical interconnect architectures.

The ultrafast laser writing technique is an alternative way to fabricate waveguide structures in bulk optical substrates with proven optical properties.[9] With this technique, it is possible to form three-dimensional (3D) structures and waveguides in arbitrary arrangements.[10] This fabrication approach has been successfully applied to produce 3D waveguide array in fused silica substrates to control spatial soliton propagation.[11,12] However, due to the small nonlinearity ($n_2 = 2.7 \times 10^{-20}$ m^2/W) in fused silica, the peak power required for nonlinear localization was reported at 1000 kW. Thus, it is highly desirable that spatial soliton waveguide arrays can be produced by ultrafast laser writing in large FOM materials such as ChGs to reduce the required intensity for switching.

Ultrafast laser writing has also been applied to waveguide fabrication in ChG. The combination of large nonlinearity and low melting point of ChG glasses leads to highly elongated and large laser modified areas,[13–15] resulting in an asymmetric multi-mode waveguide cross section, large propagation loss, and poor light confinement. The multi-pass writing scheme forms ChG waveguides

[a]Corresponding author: kchen@engr.pitt.edu

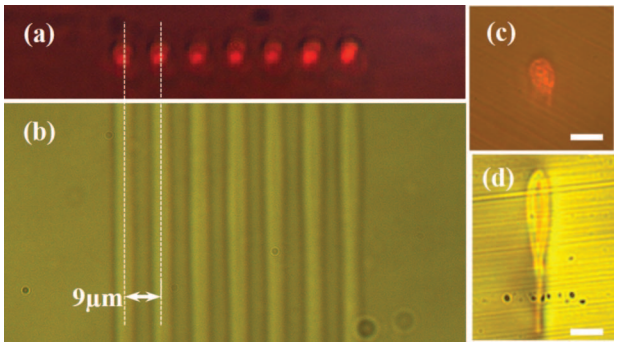

FIG. 1. Microscope images of (a) the output facet of the waveguide array; (b) the top view of the array structure; (c) symmetric waveguide cross section formed with a spatially shaped writing laser beam with a pulse width of 1.7 ps; (d) elongated waveguide cross section formed with an un-shaped writing beam with a pulse width of 300 fs. Scale bar in (c) and (d): 10 μm.

with improved symmetry in cross sections. However, the large waveguide cross-sections only support single mode operation at mid-infrared wavelengths.[16]

In this letter, we demonstrate a one-dimensional waveguide array formed in ChG substrate by ultrafast laser writing for spatial soliton all-optical switching. Both spatial beam shaping and temporal pulse tuning are employed to obtain optical waveguides with circularly symmetric cross sections to support single mode guiding at both 1040 nm (pump) and at the telecom wavelength.[17] Nonlinear optical localization in the waveguide array is demonstrated with over 70-fold reduction in switching intensity comparing to silica-based devices and 7.4 times shorter interaction distance, owing to the low waveguide loss (0.65 dB/cm), the large nonlinearity of the substrate material, and well-confined waveguide mode profiles.

The substrate material used in the experiments is the arsenic-free gallium lanthanum sulfide (GLS) ChG. In the ultrafast laser writing process, a Coherent RegA 9000 laser system operated at 800 nm with a repetition rate of 250 kHz was used for the waveguide writing. By adjusting the pulse compressing grating pairs in RegA 9000, the pulse width of the laser output was tuned to 1.7 ps for optimal processing outcomes.[17] The polarization of the laser was parallel to the laser writing direction. A cylindrical telescope was used to shape the focal volume by introducing astigmatism normal to the waveguide writing direction.[18] An 80X objective (NA = 0.75) was used to focus the laser beam at 237μm below the surface of the ChG sample. Both the temporal adjustment of laser pulse width and the spatial control of focal volumes are critical to yield waveguide arrays with desired characteristics in terms of guided mode profiles and low propagation loss. GLS glass sample with size of 10 × 10 × 2 mm^3 were used for the waveguide inscription. A three-axis motion stage (Aerotech) was used to control the laser writing pattern. All waveguides were written at a rate of 2.4 mm/s. A one dimensional waveguide array in ChG that consists of seven 1-cm long waveguides with a 9-um separation is formed. Figs. 1(a) and 1(b) show the microscope images of the output facet of the waveguide array and the array structure. With astigmatic beam shaping and temporal pulse tuning, symmetric waveguide cross section (Fig. 1(c)) is obtained in this highly nonlinear material, while an un-shaped writing beam with transform-limited pulses at 300 fs results in an elongated waveguide cross section (Fig. 1(d)).

Light propagation through the ChG waveguide array was studied using the IMPULSE^{TM} femtosecond laser system that generates pulses centered at 1040 nm with a repetition rate of 200 kHz. The pulses are sent through a pair of parallel gratings to tune its pulse width to 300 fs. An aspheric lens with f = 13.86mm, NA = 0.18 is used to launch laser pulses into the center waveguide in the array. The outputs from all waveguides are collected and collimated using another aspheric lens with f = 4.51 mm, NA = 0.55, and are imaged on a CMOS camera via a lens with 300-mm focal length.

As a reference, an individual waveguide is also formed using the same writing parameters, and characteristics of light propagation is first tested in this waveguide. The cross section of the waveguide is measured to be 5.9 × 6.3 μm^2, and its insertion loss and mode profile are measured

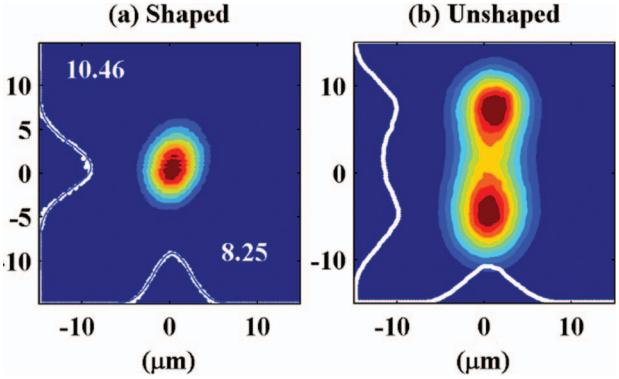

FIG. 2. Guided mode profiles of an individual waveguide (a) formed with spatially shaped writing beam; (b) formed with un-shaped writing beam.

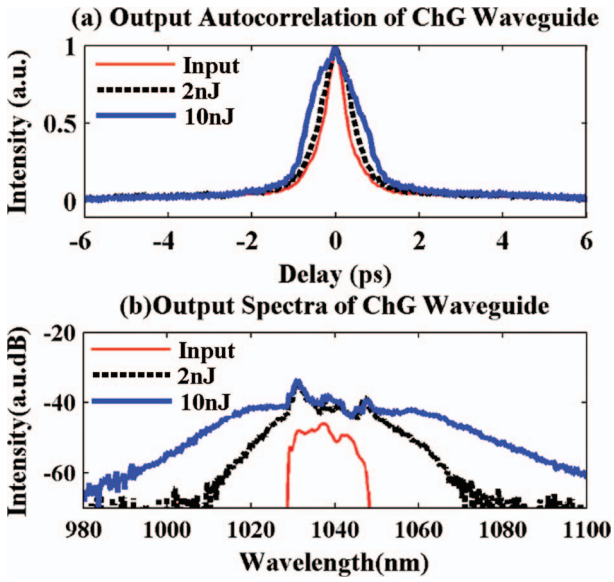

FIG. 3. (a) Autocorrelation traces and (b) output spectra of individual waveguide outputs with input pulse energies of 2nJ and 10nJ.

for light propagation at 1040 nm. The insertion loss of the waveguide is 4.43 dB, which includes 1.5 dB reflection loss from the input and output facets of the ChG substrate, 0.65 dB propagation loss, and an estimated coupling loss of 2.28 dB. Fig. 2(a) shows its guided mode profile at 1040 nm. ChG waveguides formed with a spatially shaped writing beam at 1.7-ps pulse duration support only one confined mode. The mode field diameters ($1/e^2$ diameters) are found by Gaussian fitting of the intensity profile, with 10.46 μm along the writing beam direction, and 8.25μm in the orthogonal direction. As a comparison, without spatial beam shaping or temporal pulse tuning, the resulted waveguide with elongated modified area (Fig. 1(d)) has two guiding areas and supports a much less confined guided mode profile, as shown in Fig. 2(b).

The laser pulse duration after propagation through the waveguide is also measured by a custom-built autocorrelator. The auto-correlation measurement results from an individual waveguide output are shown in Fig. 3(a) for 2-nJ and 10-nJ input pulses at 300 fs. Although the pulses experience normal group velocity dispersion (GVD) in ChG at the 1040-nm, due to the short propagation length, the laser pulses are preserved through the ChG waveguide. 12% and 40% pulse broadening were observed for 2-nJ and 10-nJ pulses, respectively. Significant frequency chirp imposed on the pulse

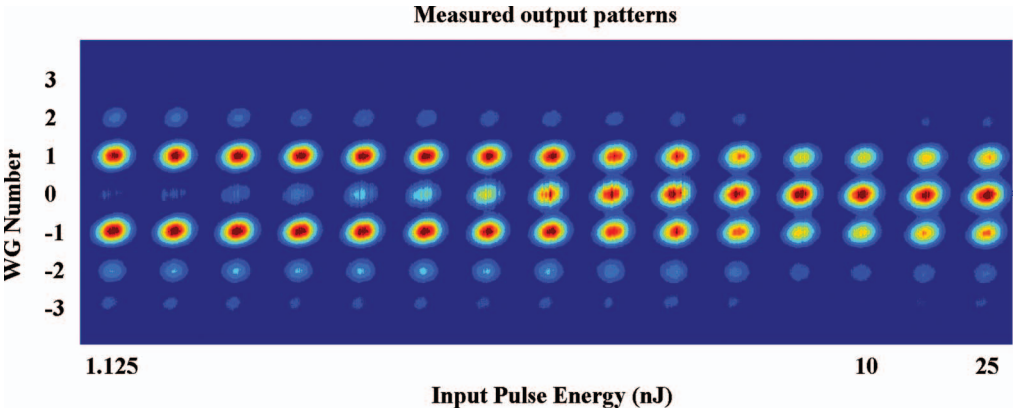

FIG. 4. Evolution of waveguide array outputs with increasing input pulse energy.

by self-phase modulation appears to be the cause of the increased pulse broadening at higher pulse energy, which is evident in the output spectra measurements shown in Fig. 3(b).

To observe nonlinear optical localization, the pump pulses are tuned to 300 fs in width and launched into the center waveguide of the array. With the input pulse energy ranging from 1.125 nJ to 25 nJ, the output patterns of the ChG waveguide array were imaged by a CMOS camera and presented in Fig. 4.

At low input pulse energies, pulse propagation through the waveguide array is dominated by linear diffraction. With only the center waveguide excited, the input power launched to the center waveguide is dissipated among the adjacent waveguides by evanescent wave coupling. The output power distribution shown in Fig. 4 is slightly asymmetric about the center waveguide, probably due to writing conditions for the symmetric waveguides are not identical due to the different orders of laser writing in the fabrication process.

With the increased input pulse energy, the optical localization becomes prominent as the nonlinear self-focusing gradually overcomes the linear diffraction, as shown in Fig. 4. The fractional optical power retained in the center waveguide increases from 3.8% to 44.5% when the input pulse energy changes from 1.125 nJ to 10 nJ. Considering the 40% broadening of pulse width at 10-nJ, the peak intensity for maximum nonlinear localization in the 1-cm long ChG waveguide array is estimated at 35.1 GW/cm^2. This is over 70-times less than the peak intensity required to achieve nonlinear localization in a 7.4-cm long waveguide array fabricated by the ultrafast laser in fused silica.[11,12]

When the input pulse energy exceeds 10-nJ, the fractional optical power retained in the center waveguide starts to decrease as shown in Fig. 4. This is probably due to the two-photon absorption of ChG at 1040 nm. Although negligible at 1550 nm, considerable two photon absorption in ChG is present for the 1040-nm laser pulses used in the experiment. This is confirmed by the numerical simulation shown in Fig. 5.

To validate the experiment results, nonlinear optical propagation in the ChG waveguide array was numerically simulated. The evolution of the electrical field in each waveguide in the array can be described by a set of coupled mode equations.[19] With the presence of the nonlinear Kerr effect, the two-photon absorption, and the linear attenuation, the equation for the electrical field E_n in the nth waveguide can be described as,

$$i{}^{dE_n}\!/_{dz} = \beta E_n + \kappa\left(E_{n+1} + E_{n-1}\right) + \gamma\left|E_n\right|^2 E_n - i\left(\alpha_1 + \alpha_2\left|E_n\right|^2\right) E_n \qquad (1)$$

where β is the propagation constant, κ is the coupling coefficient between adjacent waveguides, α_1 and α_2 are the coefficients corresponding to the linear and nonlinear waveguide loss, and γ is the nonlinear parameter that describes the Kerr nonlinearity in the waveguide. The linear attenuation $\alpha_1 = 0.65$ dB/cm, is the propagation loss in the ChG waveguide.[17] The coupling coefficient κ is 115 m^{-1}, which was determined experimentally by the output power distribution of the waveguide array in the linear propagation regime.[11]

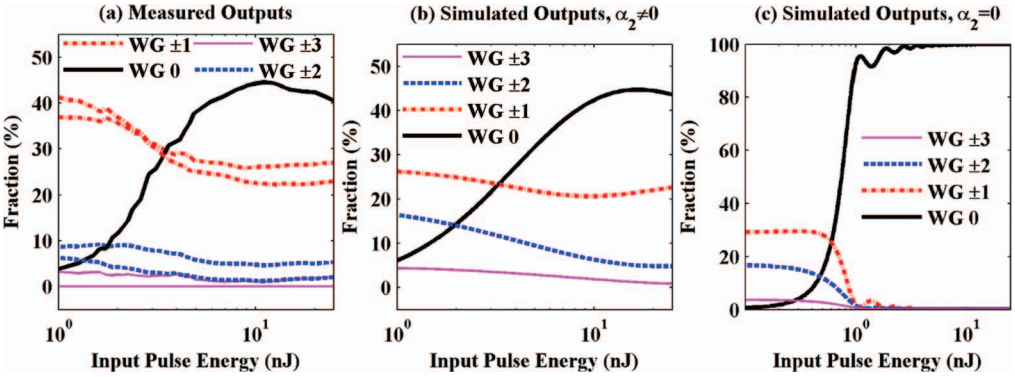

FIG. 5. Fractional powers of outputs from ChG waveguide array. (a) Measured results; (b) Simulated results with two photon absorption; (c) Simulated results without two photon absorption.

Both experimental results and simulation of the ChG waveguide array output as the function of input pulse energy are presented in Fig. 5. The measured fractional powers of each waveguide output in the array are shown in Fig. 5(a) while the simulation results are shown in Figs. 5(b) and 5(c).

The purpose of the simulation is to understand why 100% nonlinear optical localization was not achieved in the experiment and the fractional optical power retained in the center waveguide decreased at higher pulse energy as shown in Fig. 4. The nonlinear refractive index n_2 and two-photon absorption coefficient α_2 at 1040 nm for GLS glasses were used to best fit the experimental results shown in Fig. 5(a). The nonlinear refractive index n_2 at 1040 nm used to produce the simulation results shown in Fig. 5(b) is slightly larger than the reported value (2.16×10^{-18} m^2/W) measured at 1550 nm.[20]

Figures 5(b) and 5(c) compare the effect of the two-photon absorption on the device performance. Simulation results shown in Fig. 5(b) were obtained using the two-photon absorption coefficient $\alpha_2 = 0.105$ W^{-1}m^{-1}, while Fig. 5(c) shows the simulation results with no two-photon absorption ($\alpha_2 = 0$) but identical n_2. It is clear that a complete nonlinear optical localization can be achieved at reduced input pulse energy if the two-photon absorption can be ignored. Fig. 5(b) also shows that the two-photon absorption is the cause of reduced optical localization at high input pulse energy (E > 10 nJ), which is consistent with the experimental observations shown in Fig. 4 and Fig. 5(a).

In summary, nonlinear optical localization is realized in a one dimensional waveguide array. Using temporal pulse tuning and spatial laser beam shaping, symmetric nonlinear waveguide arrays that preserve the large intrinsic material nonlinearity was realized by the ultrafast laser writing technique. Light propagation in the ChG waveguide array is studied with near infrared laser pulses centered at 1040 nm. The peak intensity required to achieve the maximum nonlinear localization for the 1-cm long waveguide array was 35.1 GW/cm^2, which is 70 times lower than that reported in fused silica waveguide arrays and with over 7 times shorter interaction distance. The comparison between the experimental results and the theoretical simulations also suggest that the waveguide array could achieve better performance at 1550 nm while two-photon absorption is negligible. Results reported in this paper demonstrated that ultrafast laser writing is a viable tool to produce 3D all-optical switching waveguide circuits in chalcogenide glasses.

[1] M. Heinrich, R. Keil, F. Dreisow, A. Tünnermann, A. Szameit, and S. Nolte, Appl. Phys. B **104** (3), 469 (2011).
[2] R. Keil, M. Heinrich, F. Dreisow, T. Pertsch, A. Tunnermann, S. Nolte, D. N. Christodoulides, and A. Szameit, Sci. Rep. **1** (2011).
[3] B. J. Eggleton, B. Luther-Davies, and K. Richardson, Nat. Photon. **5**(3), 141 (2011).
[4] V. Ta'eed, N. J. Baker, L. Fu, K. Finsterbusch, M. R. E. Lamont, D. J. Moss, H. C. Nguyen, B. J. Eggleton, D.-Y. Choi, S. Madden, and B. Luther-Davies, Opt. Express **15**(15), 9205 (2007).
[5] M. Chauvet, G. Fanjoux, K. P. Huy, V. Nazabal, F. Charpentier, T. Billeton, G. Boudebs, M. Cathelinaud, and S.-P. Gorza, Opt. Lett. **34**(12), 1804 (2009).
[6] V. G. Ta'eed, M. Shokooh-Saremi, L. B. Fu, I. C. M. Littler, D. J. Moss, M. Rochette, B. J. Eggleton, Y. L. Ruan, and B. Luther-Davies, IEEE J. Sel. Top. Quantum Electron. **12**(3), 360 (2006).

[7] S. J. Madden, D. Y. Choi, D. A. Bulla, A. V. Rode, B. Luther-Davies, V. G. Ta'eed, M. D. Pelusi, and B. J. Eggleton, Opt. Express **15**(22), 14414 (2007).
[8] M. Galili, J. Xu, H. C. Mulvad, L. K. Oxenløwe, A. T. Clausen, P. Jeppesen, B. Luther-Davies, S. Madden, A. Rode, D.-Y. Choi, M. Pelusi, F. Luan, and B. J. Eggleton, Opt. Express **17**(4), 2182 (2009).
[9] K. M. Davis, K. Miura, N. Sugimoto, and K. Hirao, Opt. Lett. **21**(21), 1729 (1996).
[10] R. R. Gattass and E. Mazur, Nat. Photon. **2**(4), 219 (2008).
[11] A. Szameit, D. Blömer, J. Burghoff, T. Schreiber, T. Pertsch, S. Nolte, A. Tünnermann, and F. Lederer, Opt. Express **13**(26), 10552 (2005).
[12] A. Szameit, J. Burghoff, T. Pertsch, S. Nolte, A. Tünnermann, and F. Lederer, Opt. Express **14**(13), 6055 (2006).
[13] N. D. Psaila, R. R. Thomson, H. T. Bookey, S. Shen, N. Chiodo, R. Osellame, G. Cerullo, A. Jha, and A. K. Kar, Opt. Express **15**(24), 15776 (2007).
[14] M. Hughes, W. Yang, and D. Hewak, Appl. Phys. Lett. **90**(13), 131113 (2007).
[15] J. E. McCarthy, H. T. Bookey, N. D. Psaila, R. R. Thomson, and A. K. Kar, Opt. Express **20**(2), 1545 (2012).
[16] A. Ródenas, G. Martin, B. Arezki, N. Psaila, G. Jose, A. Jha, L. Labadie, P. Kern, A. Kar, and R. Thomson, Opt. Lett. **37**(3), 392 (2012).
[17] B. McMillen, B. Zhang, K. P. Chen, A. Benayas, and D. Jaque, Opt. Lett. **37**(9), 1418 (2012).
[18] R. Osellame, S. Taccheo, M. Marangoni, R. Ramponi, P. Laporta, D. Polli, S. De Silvestri, and G. Cerullo, J. Opt. Soc. Am. B **20**(7), 1559 (2003).
[19] H. S. Eisenberg, Y. Silberberg, R. Morandotti, A. R. Boyd, and J. S. Aitchison, Phys. Rev. Lett. **81**(16), 3383 (1998).
[20] J. Requejo-Isidro, A. K. Mairaj, V. Pruneri, D. W. Hewak, M. C. Netti, and J. J. Baumberg, J. Non-Cryst. Solids **317**(3), 241 (2003).